Electronic Supplementary Material (ESI) for Journal of Materials Chemistry B.

Supporting Information

DNA Nanotubes in Coacervate Microdroplets as Biomimetic Cytoskeletons Modulate the Liquid Fluidic Properties of Protocells

Shaohong Zhou, Xueer Cai, Yanwen Zhang, Qiaoshu Chen, Xiaohai Yang, Kemin Wang, Lixin Jian, and Jianbo Liu**

State Key Laboratory of Chemo/Biosensing and Chemometrics, College of Chemistry and Chemical Engineering, Key Laboratory for Bio-Nanotechnology and Molecular Engineering of Hunan Province, Hunan University, Changsha 410082, P. R. China.

Email: jlxyx@hnu.edu.cn, liujianbo@hnu.edu.cn

SI Figures

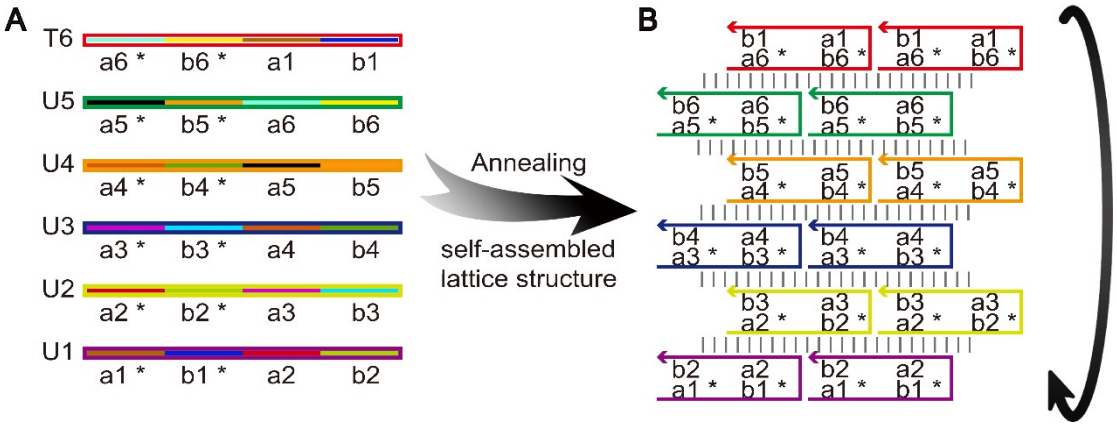

Figure S1. (A) The 42-nucleotide (nt) single-stranded DNA motif has four concatenated modular domains: Different colors represent different modules， modules of the same color are complementary chains, for example, a1 and a1* are complementary strands. (**B**) The DNA secondary structure is self-assembled by annealing and complementary hybridization.

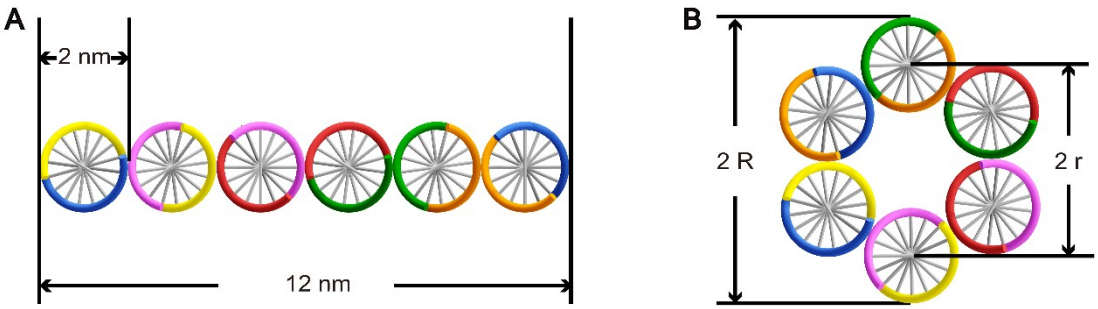

Figure S2. Calculation method of DNA nanotube diameter (cross-section view): (A) The diameter of each double helix DNA is set to 2 nm, then the 6-helix ribbon length is 12 nm (six double helix DNA). (**B**) The circumference of the inner circle of the synthesized DNA nanotube is 12 nm, $2r = 12 / \pi$ nm = 3.8 nm, and the diameter of the outer circle is $2R = 2r + 2 = 5.8$ nm. Therefore, the diameter of the DNA nanotube is approximately 5.8 nm. The design of DNA sequences and the calculation of DNA nanotube diameter were conducted according to a previous report (Yin, P., et. al. (2008) Science 321, 824-826).

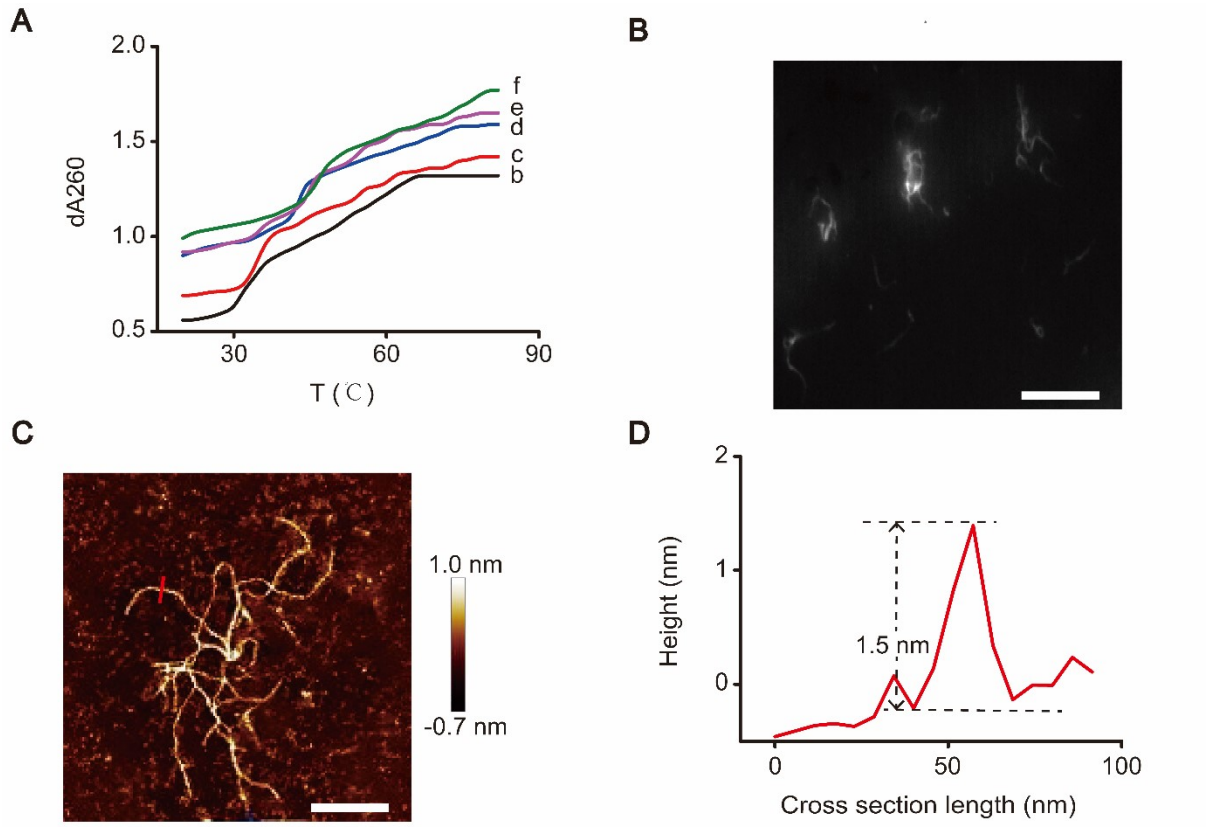

Figure S3. Characterization of 5-helix nanoribbons. (**A**) Negative first derivative of the melting curves of DNA nanostructures: 2-helix nanoribbons (b), 3-helix nanoribbons (c), 4-helix nanoribbons (d), 5-helix nanoribbons (e), 6-helix nanotubes (f). (**B**) TRIF imaging of the DNA 5-helix nanoribbons. Scale bar: 10 μm; (**C**) AFM imaging of the 5-helix nanoribbons. Scale bar: 2.5 μm. (**D**) Line profile of a cross section in the AFM imaging in panel (**C**), Height is 1.5 nm.

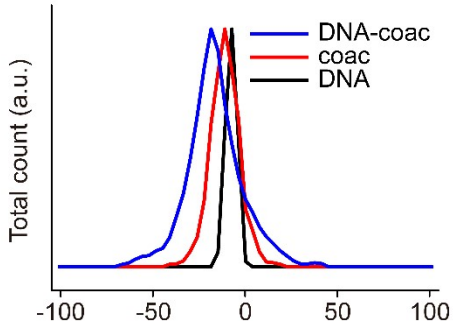

Figure S4. Zeta potentials of DNA, DNA nanotubes, and DNA nanotube-containing coacervate microdroplets.

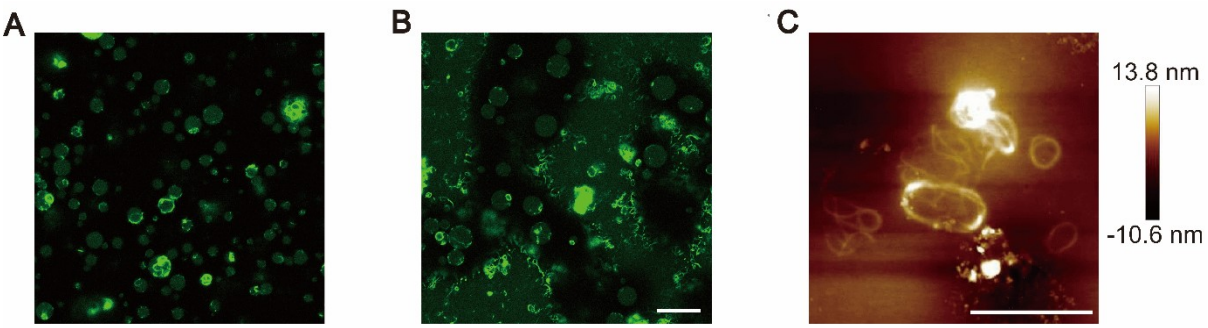

Figure S5. (**A**) Confocal fluorescence images of DNA nanotubes-containing coacervate microdroplets. Fluorescence imaging (**B**) and AFM imaging (**C**) of DNA nanotubes after the nanotubes-containing coacervate microdroplets dissociated in 20× deionized water. Scale bars, 2 μm.

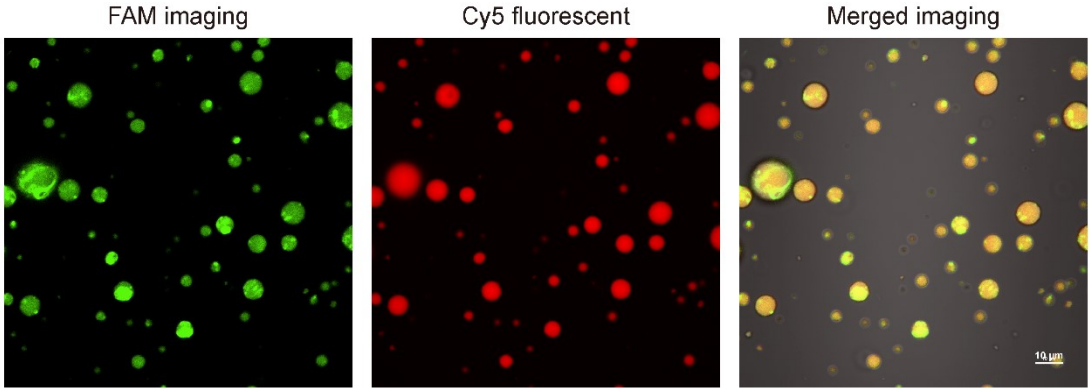

Figure S6. Fluorescent imaging of coacervate microdroplets after incubation with Cy5 for 10 min. Scale bar: 10 μm.

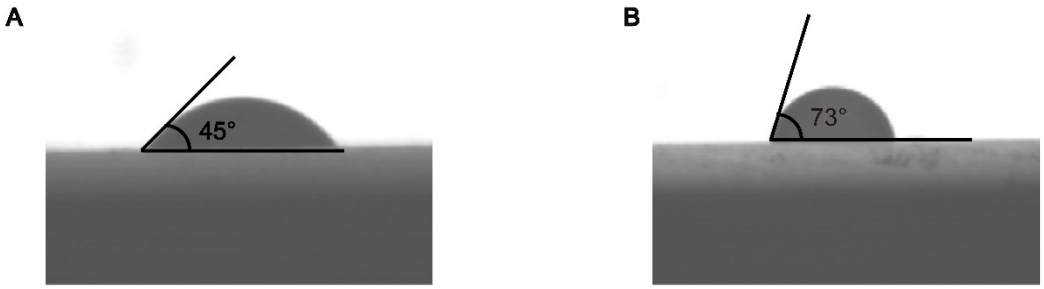

Figure S7. Contact angle of DNA nanotube-free (**A**) and nanotube-containing (**B**) coacervate microdroplets, which was determined to be 45° and 73°, respectively.

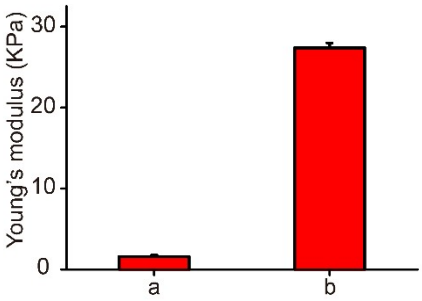

Figure S8. Young's modulus of DNA nanotube-free (**a**) and nanotube-containing (**b**) coacervate microdroplets, which was calculated to be 1.6 ± 0.2 KPa and 27.4 ± 0.6 KPa, respectively. (n=3).

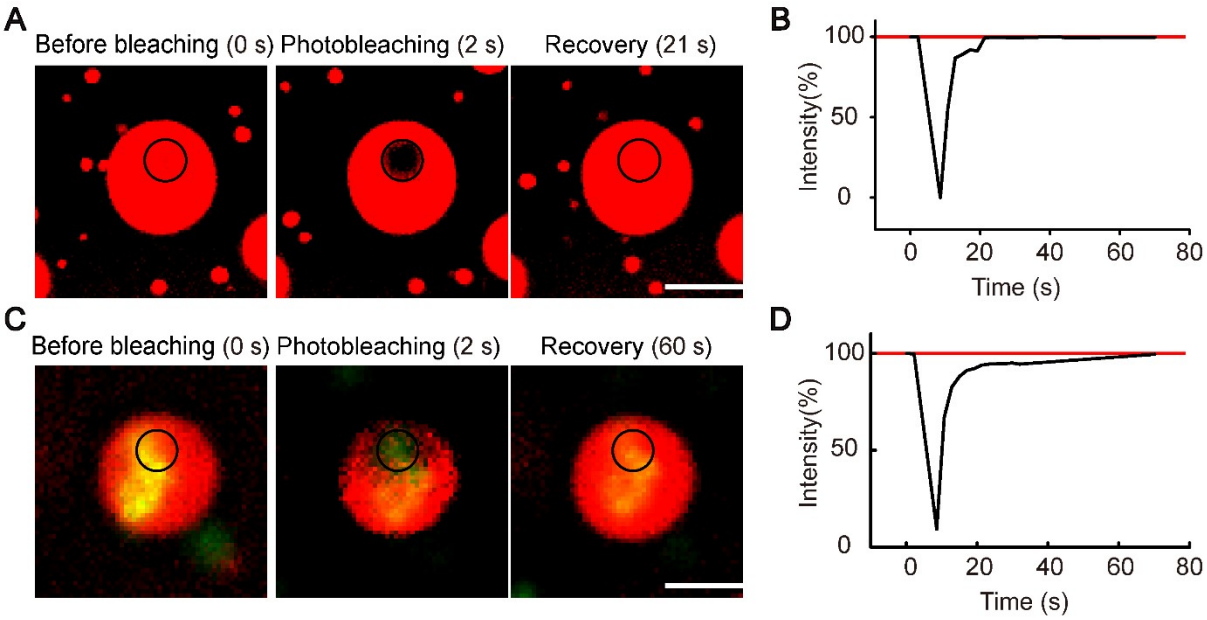

Figure S9. FRAP measurements of liquid fluidity in DNA nanotube-free (A) and nanotube-containing (C) coacervate microdroplet. Time series of confocal fluorescence images of a single DNA nanotube-free coacervate microdroplets with Cy5-HRP (A) and corresponding time-dependent changes in coacervate microdroplet fluorescence intensity (B) recorded before (left), 2 s after the onset of photobleaching (middle, high laser power) and 80 s after recovery (right, low laser power). The photobleached area is delineated by the black circle in (A) and corresponds to the black line in (B). (C and D) As for (A and B) but for a single nanotube-containing coacervate microdroplet; note the considerably longer recovery time due to decreased microdroplets fluidity. Scale bars, 5 μm.

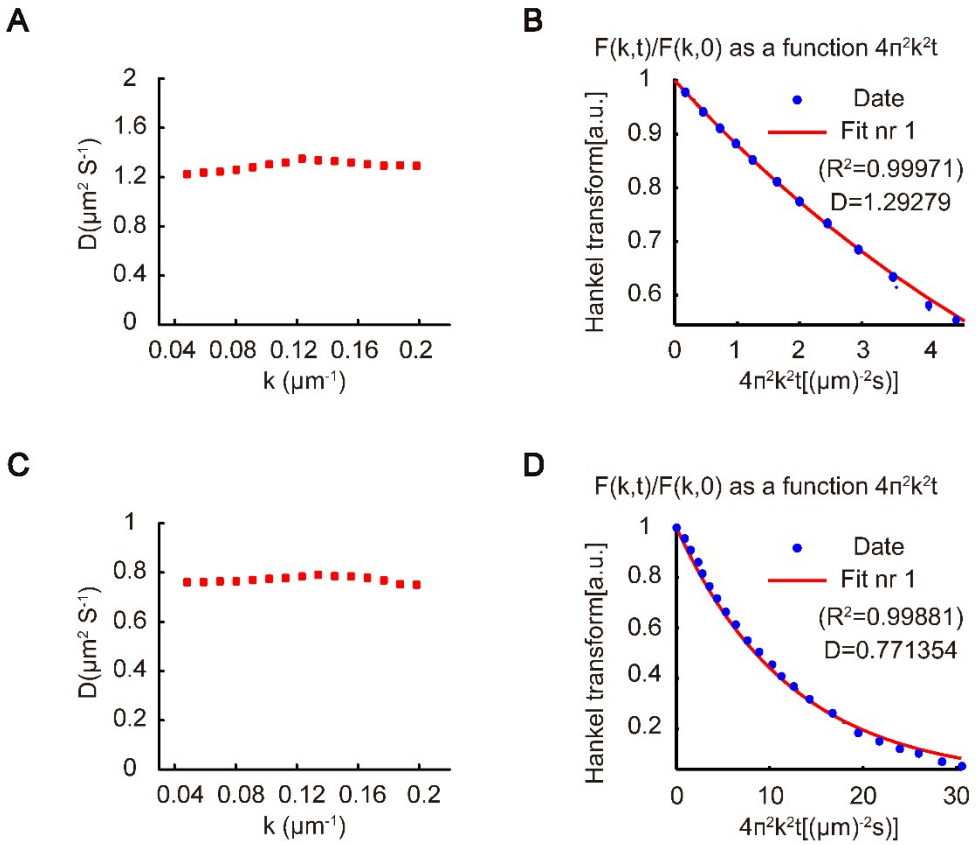

Figure S10. (A, C) Plots showing the diffusion coefficient values (D(k)) determined at each individual value of the spatial frequency (k) for the single DNA nanotube-free (A) and nanotube-containing (C) coacervate microdroplet shown in Figure S9. (A, C) Graphs showing curve fittings for F(k,t)/F(k,0) vs $4\pi^2 k^2 t$ for the DNA nanotube-free (B) and nanotube-containing (D) coacervate microdroplet.

Table S1 Oligonucleotide sequences (from 5' to 3') used in this work. * indicates the complementarity strand (for example, a1 and a1* are complementary strands).

Seq_ID	Domains	Sequence (from 5′ to 3′)
U1	a1*-b1*-a2-b2	GGCGATTAGG-ACGCTAAGCCA-CCTTTAGATCC-TGTATCTGGT
U2	a2*-b2*-a3-b3	GGATCTAAAGG-ACCAGATACA-CCACTCTTCC-TGACATCTTGT
U3	a3*-b3*-a4-b4	GGAAGAGTGG-ACAAGATGTCA-CCGTGAGAACC-TGCAATGCGT
U4	a4*-b4*-a5-b5	GGTTCTCACGG-ACGCATTGCA-CCGCACGACC-TGTTCGACAGT
U5	a5*-b5*-a6-b6	GGTCGTGCGG-ACTGTCGAACA-CCAACGATGCC-TGATAGAAGT
T6	a6*-b6*-a1-b1	GGCATCGTTGG-ACTTCTATCA-CCTAATCGCC-TGGCTTAGCGT
FAM-U1	a1*-b1*-a2-b2	/FAM/TT- GGCGATTAGG-ACGCTAAGCCA-CCTTTAGATCC-TGTATCTGGT